Journal of Sol-Gel Science and Technology 30, 157–161, 2004

The Optical Properties of ZnO Nanoparticles Capped with Polyvinyl Butyral

Y.H. TONG
Center for Advanced Opto-Electronic Functional Material Research, Northeast Normal University, Changchun 130024, People's Republic of China

Y.C. LIU*
Center for Advanced Opto-Electronic Functional Material Research, Northeast Normal University, Changchun 130024, People's Republic of China; Key Lab. of Excited State Process, Chinese Academy of Sciences; Changchun Institute of Optics, Fine Mechanics and Physics, Changchun 130021, People's Republic of China
ycliu@nenu.edu.cn

S.X. LU AND L. DONG
Key Lab. of Excited State Process, Chinese Academy of Sciences; Changchun Institute of Optics, Fine Mechanics and Physics, Changchun 130021, People's Republic of China

S.J. CHEN
Center for Advanced Opto-Electronic Functional Material Research, Northeast Normal University, Changchun 130024, People's Republic of China

Z.Y. XIAO
Key Lab. of Excited State Process, Chinese Academy of Sciences; Changchun Institute of Optics, Fine Mechanics and Physics, Changchun 130021, People's Republic of China

Received August 20, 2003; Accepted April 20, 2004

Abstract. ZnO nanoparticles capped with polyvinyl butyral (PVB) have been synthesized by the sol-gel process. Photoluminescence (PL) spectra show a remarkable decrease in visible emission intensity after ZnO nanoparticles are capped with PVB, which indicates that dangling bonds and defect states at the surface of ZnO nanoparticles are markedly passivated. As a result, the process of surface-trapped hole tunneling back into the particles to form V_O^{**} recombination center is blocked. The PL spectra of thin films show a strong ultraviolet (UV) emission with very weak visible emission. The typical intensity ratio of the UV emission at 3.45 eV to the visible emission at about 2.41 eV is 43.3, which shows an obvious improvement in luminescence properties by the surface passivation with PVB. Low-temperature PL spectra of ZnO powder at 93.8 K are dominated by free exciton, bound exciton and the LO-phonon replica of the bound exciton.

Keywords: nanoparticle, ZnO, polyvinyl butyral, surface passivation, photoluminescence

*To whom all correspondence should be addressed.

1. Introduction

Semiconductor nanoparticles are receiving much attention owing to their novel physical and chemical properties. In comparison with the bulk semiconductor, semiconductor nanoparticles possess many special properties such as ultrafast optical nonlinear response, photoelectricity switch and piezoelectric properties. At present, the high-speed development of biotechnology, energy sources, environment and advanced manufacture technology urgently require to obtain material miniaturization, intelligentization, high integration and high density transmission, which offer a broad application for semiconductor nanoparticles. Recently, the preparation of some semiconductor nanoparticles including CdSe, CdS and ZnS has been quite perfect [1–5]. In addition, their shapes and sizes can also be well controlled. However, there has not been an equivalent success in the synthesis of metal oxide nanoparticles such as ZnO nanoparticles because of the complexity of hydrolyzation in metal ion. ZnO nanoparticles do not only have the merits of ZnO semiconductor material such as a large exciton binding energy of 60 meV and excellent stability, but also have some novel characteristics because of the particularity of nanostructure. ZnO nanoparticles have attracted much attention due to the strong commercial desire for photocatalysis, photoelectrochemistry, blue and ultraviolet (UV) light emitters and detector. However, it is well known that small particles have the large surface-to-volume ratio and surface defects. The photoluminescence (PL) spectra of most ZnO nanoparticle samples showed a near-band-edge (NBE) UV line accompanied by a strong visible luminescence, which can result in a decrease in carrier/exciton lifetime and emission efficiency in the UV light devices. So the most crucial aspects of high luminescence efficiencies from ZnO nanoparticles are the surface texture and an efficient surface passivation. Fortunately, polymer capping can effectively passivate the surface of nanoparticles and reduce the surface-related visible emission [6].

In this paper, we report in detail the synthesis of ZnO nanoparticles capped with polyvinyl butyral (PVB) by the sol-gel process. The sol-gel technique is known to have many distinct merits such as process simplicity and high homogeneity, which offers the possibility of large-area yield at low cost and low temperature synthesis for technological application. In order to investigate the effect of PVB on the optical properties, both powder sample and film sample were obtained. Surface passivation of ZnO nanoparticles via PVB markedly enhances UV emission and decreases visible luminescence. The mechanism of the surface passivation is also discussed.

2. Experimental Details

Lithium hydroxide monohydrate ($LiOH{\cdot}H_2O$) was purchased from Aldrich. Zinc acetate dihydrate ($Zn(CH_3COO)_2{\cdot}2H_2O$) and all the solvents were purchased from Beijing Chemicals Co. Ltd. Ethanol was dehydrated by Lund and Bjezzum's method, utilizing the reactions with magnesium ethoxide [7].

The synthesis was performed by the following method: 2.7 wt.% $Zn(CH_3COO)_2$ was first dissolved to a saturated solution of PVB in absolute ethanol. Then 0.73 wt.% LiOH solution in absolute ethanol was added, with vigorous stirring at 50°C. Aliquots of sol were taken out at the interval of 20 minutes and 40 minutes for absorption spectra measurements and PL measurements. The thin films were fabricated by multiply dip-coating of the resulting zinc oxide sol onto silicon wafers. Finally, the nanoparticles were precipitated using hexane at 40 minutes. After the supernatant was removed, the wet precipitate was shelved at air atmosphere for days and the white powder was obtained.

The structure of ZnO nanoparticles was charaterized by X-ray diffraction using D/max-rA X-ray diffraction spectrometer (Rigaku) with a Cu K_α of 1.54 Å. The PL spectra were measured using the He-Cd laser operating at a wavelength of 325 nm with 40 mW. The absorption spectra of ZnO sol were obtained by UV-360 Spectrophotometer (Shimadzu).

3. Results and Discussion

Figure 1 shows X-ray diffraction spectra of the powders with and without capping PVB. There are seven diffraction peaks for two samples, which correspond to (100), (002), (101), (102), (110), (103) and (112) diffraction peaks of hexagonal wurtzite structure ZnO, respectively. The particle size D can be calculated using the Debye-Scherrer formula:

$$D = \frac{0.9\lambda}{B\cos\theta_B},$$

where λ is the x-ray wavelength (1.54 Å), θ_B is the Bragg diffraction angle, and B is the full width at half

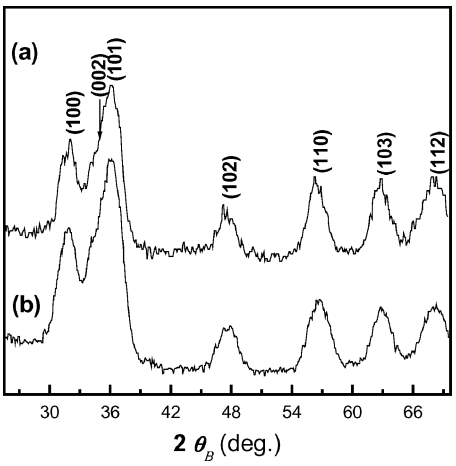

Figure 1. X-ray diffraction patterns of the uncapped powder (a) and the capped powder (b) with molecules PVB.

maximum. According to the seven diffraction peak positions and the widths at half maximum, the mean sizes of ZnO nanoparticles obtained are 3.82 nm and 4.36 nm for the uncapped and capped powders, respectively. This result indicates that PVB does not obviously influence on the structure and the size of ZnO nanoparticles.

Figure 2 shows the PL spectra of the powders with and without capping PVB. Both PL spectra consist of UV emission and visible emission. But the relative intensity of two emission peaks varies. The UV emission is significantly enhanced while the visible emission decreases drastically for the ZnO nanoparticles capped with PVB. The strong UV luminescence obtained results from the surface passivation. Generally, the UV emission is attributed to the exciton radiative recombination while that of the visible emission remains uncertain. In the past 40 years, various mechanisms have been proposed [8–10]. Until recently, Dijken et al. figured that the particle surface played an important role in the visible emission [11]. They offered a model: The valence band hole can be trapped by surface states and then tunnels back into oxygen vacancies containing one electron (V_O^*) to form V_O^{**} recombination center. The recombination of a shallowly trapped electron with a deeply trapped hole in a V_O^{**} center causes visible emission. For the uncapped ZnO nanoparticles, the existence of abundant surface defects results in the strong visible emission, as shown in Fig. 2(a). For ZnO nanoparticles, there are many oxygen or zinc defects (dangling bonds) at the grain boundaries. These oxygen defects facilitate the conjugation with hydroxyl of PVB molecule by hydrogen bonding. Furthermore, the zinc defects at the interface adsorb oxygen, which can also combine with hydroxyl of PVB molecule. As a result, the interface defects decrease, and the probability of surface trapped hole is decreased. At the same time, PVB molecules spatially block the process of surface-trapped hole tunneling back into the particles to form V_O^{**} center. Both effects lead to decreasing the probability of V_O^{**} recombination (visible emission). Therefore, in comparison with the uncapped ZnO nanoparticles, the visible emission of ZnO nanoparticles capped with PVB becomes very weak. Furthermore, a nonradiative recombination process at the surface is also considered [11]. In the case of ZnO nanoparticles, a photogenerated electron in the conduction band gets trapped at the surface and recombines with the surface-trapped hole resulting in the nonradiative recombination. When the surface is passivated via PVB capping, the probability of nonradiative recombination at the surface of nanoparticles decreases. In general, radiative trap recombination, nonradiative recombination and radiative exciton recombination are three competition processes. Decreasing in the probabilities of the former two processes eventually leads to increasing the intensity of the UV PL peak when the nanoparticles are capped with PVB.

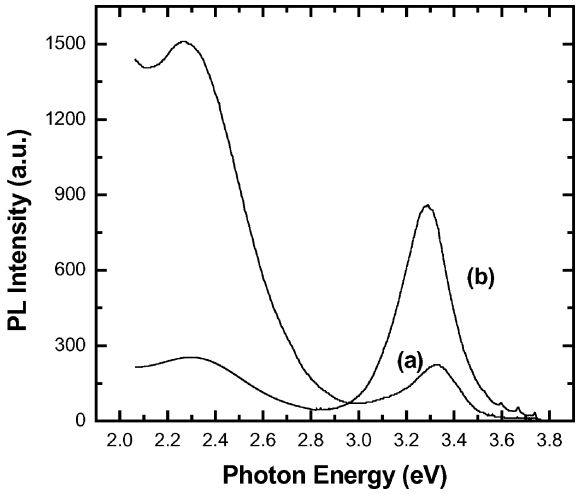

Figure 2. Photoluminescence spectra of the uncapped powder (a) and the capped powder (b) with molecules PVB.

In addition to the powder PL spectra, the PL spectra of thin films obtained by the multiple coating procedure are also investigated. Figure 3 shows the PL spectra (solid line) and the optical absorption spectra (dotted

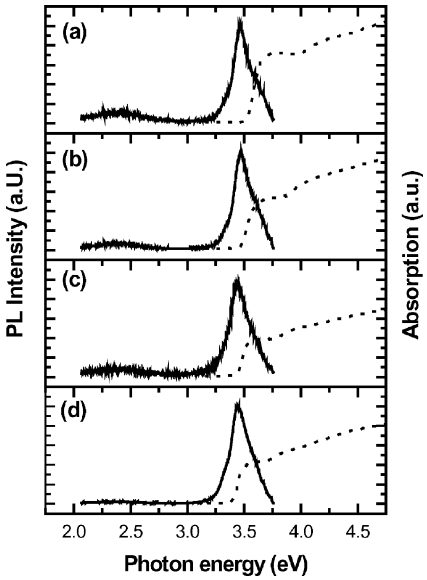

Figure 3. Photoluminescence spectra (solid line) and optical absorption spectra (dotted line) of different ZnO nanoparticles: (a) the uncapped nanoparticle thin films coated by the sol stirred for 20 minutes, (b) the capped nanoparticle thin films coated by the sol stirred for 20 minutes, (c) the uncapped nanoparticle thin films coated by the sol stirred for 40 minutes, (d) the capped nanoparticle thin films coated by the sol stirred for 40 minutes.

line) of different ZnO nanoparticles. Here, Figs. 3(a) and (b) are the uncapped and capped thin films coated by the sol stirred for 20 minutes, Figs. 3(c) and (d) are the uncapped and capped nanoparticle thin films for 40 minutes. As shown in Figs. 2 and 3, the visible emission of thin films is obviously weaker than that of powders because Si substrate provides circumstances of surface molecule transportation and configuration variation during the process of sol drying, which dramatically decrease surface defects. For the nanoparticles with and without PVB capping for the same aging time, it is obvious that both the UV emission peak position and the absorption edge do not vary, which derives from the little variety of the mean particle size. However, the particle size increases with the aging time, as evidenced by the red shifts of the UV emission peak and the absorption edge. When the ZnO nanoparticles are capped with PVB, the visible emission decreases. Moreover, the visible emission of ZnO nanoparticle thin film with PVB capping for 40 minutes is almost quenched. The typical intensity ratios of the UV emission at about 3.45 eV to the visible emission at about 2.41 eV are 4.8, 14.2, 12.6 and 43.3 for a, b, c and d, respectively, which indicate that the UV PL of ZnO

Table 1. UV PL peak position and optical absorption edge position of different ZnO nanoparticles: (a) uncapped films for 20 minutes, (b) capped films for 20 minutes, (c) uncapped films for 40 minutes, (d) capped films for 40 minutes.

Units (eV)	a	b	c	d
UV PL peak position	3.468	3.472	3.436	3.444
Absorption edge position	3.605	3.563	3.523	3.467
Stokes shift	0.137	0.091	0.087	0.023

nanoparticles was obviously improved by surface passivation with PVB. According to Fig. 3, the UV PL position, absorption edge position and stokes shifts are given in Table 1. For the capped nanoparticles with PVB, there are smaller stokes shifts than those of the uncapped nanoparticles, which indicates a decrease in surface defect states as well [12]. With comparison between Figs. 2 and 3, it can be see that the peak wavelength of UV emission due to free exciton of quantum confined ZnO particles is shorter in film than in powder with the same aging time, which is because that nanoparticles tend to reunite during the process of colloid precipitation to form powder because of the van der Waals strength or the columbic interaction between nanoparticles. In fact, the interface reactions can easily be realized due to the existence of large interface defects for the nanoparticles, which leads to an increase in chemical potential to enhance interface reaction. For ZnO nanoparticles, there are many zinc or oxygen defects (dangling bonds) at the grain boundaries. These defects are favorable to the merging process, as a result of this, to form large ZnO grains.

Figure 4 shows the temperature dependence of PL spectra of the powder capped with PVB from 98.3 to 276.1 K. At low temperature, the UV PL peak is dominated by free exciton (E_{ex}), bound exciton (B_{ex}) and the LO-phonon replica of the bound exciton (B_{ex}–LO). As the temperature increases, the free exciton tends to be obvious and eventually dominates the PL spectra at about 253.3 K. All UV peaks shift to longer wavelengths from low to high temperature. The temperature dependence of the peak position of free exciton is shown in Fig. 5. We fit the data according to the following equation [13]:

$$E(T) = E(0) - \frac{\alpha T^2}{T + \beta},$$

where $E(0)$, α and β are parameters. The solid curve in Fig. 5 is the theoretical fitting to the experimental

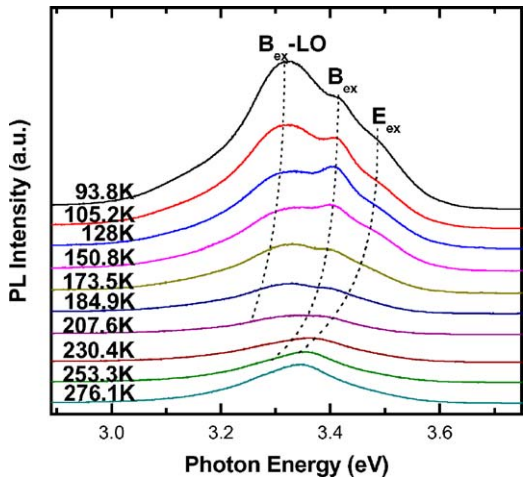

Figure 4. Temperature dependence of photoluminescence spectra of the powder capped with PVB from 98.3 to 276.1 K.

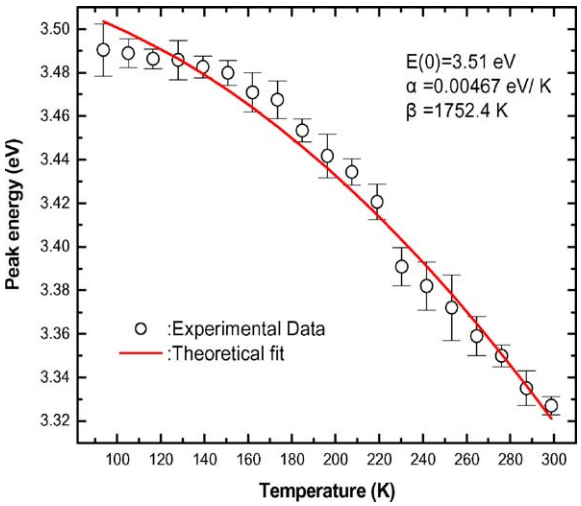

Figure 5. Free exciton peak energy as a function of temperature ranging from 93.8 to 298.9 K. The theoretical simulation (solid curve) to the experimental data points (○) is obtained using Eq.: $E(T) = E(0) - \alpha T^2/(T + \beta)$.

data for the ZnO powder. We obtain $E(0) = 3.51$ eV, $\alpha = 0.00467$ eV/K, $\beta = 1752.4$ K. The peak energy value of the free exciton is much larger than that of bulk ZnO (3.37 eV) due to the quantum confinement effect of small particle size.

In conclusion, ZnO nanoparticles capped with PVB are prepared by the sol-gel process and the particles can be obtained both in powder form and in coating film form. The influence of PVB on the optical properties of ZnO nanoparticles is investigated. When the ZnO nanoparticles are capped with PVB, PVB molecules do not only improve the surface of ZnO nanoparticles by compensating dangling bonds and unsaturated bonds, but also spatially block the process of surface-trapped hole tunneling back into the particles to form V_O^{**} recombination center. The PL spectra of powders and coating films suggest that the surface passivation via PVB capping is an effective method to improve the optical characters of ZnO nanoparticles.

Acknowledgments

This work is supported by the Program of CAS Hundred Talents, the National Natural Science Foundation of China No. 60176003, 60376009 and 60278031, the "863" Advanced Technology Research Program.

References

1. L.L. Hench and J.K. West, Chem. Rev. **90**, 33 (1990).
2. M.A. Hines and P.G. Sionnest, J. Phys. Chem. **100**, 468 (1996).
3. X. Peng, Chem. Eur. J. **8**, 335 (2002).
4. L. Li, J. Hu, W. Yang, and A.P. Alivisatos, Nano Lett. **1**, 349 (2001).
5. M. Nirmal and L. Brus, Acc. Chem. Res. **32**, 407 (1999).
6. C.L. Yang, J.N. Wang, W.K. Ge, L. Guo, S.H. Yang, and D.Z. Shen, J. Appl. Phys. **90**, 4489 (2001).
7. D.D. Perrin and W.L.F. Armarego, *Purification of Laboratory Chemicals*, 4th edition (Butterworth Heinemann, Oxford, 1997), p. 209.
8. K. Vanheusden, W.L. Warren, C.H. Seager, D.R. Tallar, J.A. Voigt, and B.E. Gnade, J. Appl. Phys. **79**, 7983 (1996).
9. Y. Li, G.W. Meng, L.D. Zhang, and F. Phillipp, Appl. Phys. Lett. **76**, 2011 (2000).
10. S.A. Studenilin, N. Golego, and M. Cocivera, J. Appl. Phys. **84**, 2287 (1997).
11. A. van Dijken, E.A. Meulenkamp, D. Vanmaekelbergh, and A. Meijerink, J. Phys. Chem. B **104**, 1715 (2000).
12. H. Fu and A. Zunger, Phys. Rev. B **56**(3), 1496 (1997).
13. H.J. Ko, Y.F. Chen, Z. Zhu, T. Yao, I. Kobayashi, and H. Uchiki, Appl. Phys. Lett. **76**, 1905 (2000).